

Etch-Back Simplifies Interdigitated Back Contact Solar Cells

Ngwe Zin, Andrew Blakers, Evan Franklin, Kean Fong, Teng Kho, Chog Barugkin and Eric Wang

Centre for Sustainable Energy Systems, Australian National University, Canberra, ACT, 0200, Australia

Abstract — The process of making Interdigitated Back Contact (IBC) solar cell is implemented by a novel simplified etch-back technique, while aiming for no compromise on high-efficiency potentials. Simplified etch-back creates localized heavy and light phosphorus and boron diffusions simultaneously. This process also leaves localised heavy diffusions to be approximately a micron higher than neighbouring light diffusion regions. In comparison to the IBC solar cells that ANU developed to date [1], key advantages of this technique feature reduction in cell process steps; requires only two diffusions to create p, p+, n and n+ diffusions; no high-temperature oxidation masking steps required as diffusion barriers; independent optimization of contact recombination, lateral carriers transport and surface passivation; and potential higher silicon bulk lifetime and reduced contamination due to low thermal budget. Based on the etch-back technique, the total saturation current density deduced from the test structures for the IBC cell is below 30 fA/cm².

Index Terms — IBC, etch-back, diffusions, solar cell, high efficiency, charge density, J_{oe} .

I. INTRODUCTION

IBC solar cells have proven to be highly efficient in lab [1-4] and commercial environments [5-7]. Besides, IBC cell structures incorporating heterojunction technology have recently achieved the outstanding efficiency [8, 9]. Despite the high efficiency potentials of IBC solar cells, the process of making them still constitutes quite a number of steps. Making IBC cell process simpler with reduced number of fabrication steps, while having no compromise on the performance of the cells, are desirable in lab or commercial environments.

In this paper different diffusion conditions are investigated to work in conjunction with etch-back. Test structures are also created to analyse diffusion profiles at different etch conditions. Recombination of etch-back assisted IBC (EB-IBC) Si solar cells following oxide passivation and nitride capping layer are also studied. Based on test results, simplified etch-back technique is applied to the cell fabrication and a new process is presented. Area-weighted recombination parameters are also extracted from the cell structure. Based on the recombination parameters, the performance of EB-IBC cells is simulated.

II. EXPERIMENTS

First, n- and p-diffusion conditions that can be implemented with etch-back are identified. Samples are grouped into A and

B. Group A has high-resistivity (>120 Ωcm) 100mm p-type FZ <100> 500 micron thick samples, while group B has n-type wafers with same wafer parameter as group A. Group A samples were first saw-damage etched and processed for a phosphorus diffusion with sheet resistance (R_{sh}) of 40 Ω/□. Samples were then grown conformally with low pressure chemical vapour deposited (LPCVD) nitride (SiN_x) of 50 nm. The purpose of LPCVD SiN_x capping is to mimic phosphorus diffusion profile from the cell process of the IBC device made at ANU [1] and to mask samples from subsequent boron diffusion. Half of group A and B samples were processed for boron diffusion with R_{sh} of 105 Ω/□, and remaining samples in group A and B were processed for boron diffusion with R_{sh} of 42 Ω/□ respectively. LPCVD SiN_x on group A samples were then removed in hydrofluoric acid (HF). 4-point probe and electrochemical capacitance-voltage (ECV) measurement techniques were used to identify R_{sh} and diffusion profiles of some group A and B samples (Figure 1).

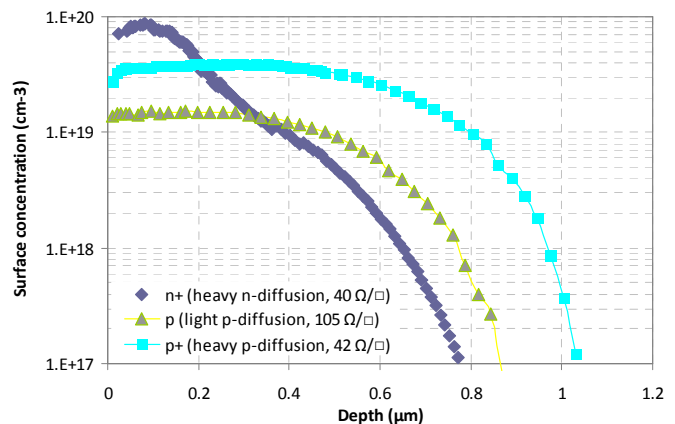


Figure 1. Phosphorus and boron diffusion profiles measured by ECV.

Samples with phosphorus and boron diffusion were then etched back concurrently in 25% concentrated tetramethylammonium hydroxide (TMAH) at ~50°C for different etch time durations. Simultaneous etch-back option on both phosphorus and boron diffusions is chosen, as simplification of the process is the key component of this paper. The etch duration is varied from 5 to 16 minutes, and R_{sh} is recorded after each etch time. Figure 2 includes different R_{sh} remained with varied etch time lengths. As in figure 2, light p-diffusion is etched off completely after 5 minutes in 50°C TMAH, while other diffused samples are still remained

with R_{sh} in the range of 160 to 530 Ω/\square , following 14 minutes of etch in TMAH.

Etch-back samples with lighter diffusion R_{sh} were then RCA cleaned and processed for oxidation at a temperature of 950°C for 25 min, followed by nitrogen drive-in at 1000°C for 30 min. Samples were then forming gas annealed at 400°C for 30 min. Photoconductance (PCD) measurement technique was used to measure saturation current densities, J_{oe} of those samples at a carrier injection of $5 \times 10^{15} \text{ cm}^{-3}$. Oxide passivated boron diffused samples have the best J_{oe} of 16 fA/cm², while phosphorus diffused samples have 10 fA/cm² (Figure 3).

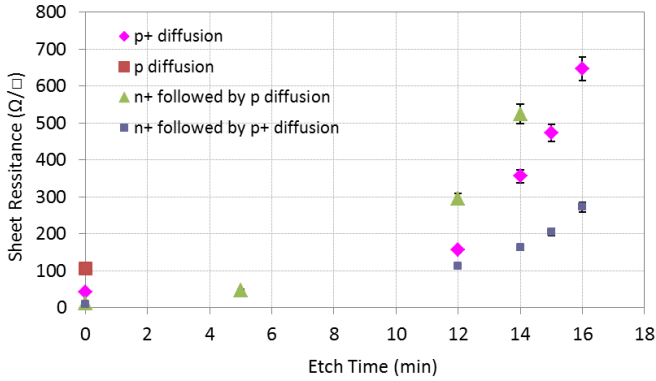


Figure 2. R_{sh} of diffused samples based on different TMAH etch time durations. P diffusion with (105 Ω/\square at 0 min) is removed completely following 5 min of etch. Boron diffused samples with 150 Ω/\square has surface concentration of $\sim 1.4 \times 10^{18} \text{ cm}^{-3}$, 350 Ω/\square has $5 \times 10^{17} \text{ cm}^{-3}$, 480 Ω/\square has $3 \times 10^{17} \text{ cm}^{-3}$ and 650 Ω/\square has $1 \times 10^{17} \text{ cm}^{-3}$, while phosphorus diffused sample with 112 Ω/\square has surface concentration of $\sim 3 \times 10^{18} \text{ cm}^{-3}$. Surface concentrations of diffusion samples are estimated from the diffusion profile.

Oxide-passivated diffused samples were then deposited with PECVD nitride ($\sim 100 \text{ nm}$, 300°C 7 min) on both front and rear. Samples were then treated in forming gas environment at 400°C for 30 min - since sharply degraded carrier lifetime of oxide passivated samples following PECVD nitride is the cause of radiation damage, which is recovered by annealing [10] - followed by measurement of J_{oe} . This is to mimic the dielectric capping layer on the rear of the IBC cell. J_{oe} of oxide-passivated boron samples (especially lightly diffused) following PECVD nitride and forming gas has increased by nearly 2-folds. However, the same is not observed for phosphorus samples. Similar increase of J_{oe} is also observed for diffused boron samples following LPCVD nitride growth. Significant increase in surface recombination of boron diffused samples after PECVD nitride could be due to excess positive charges in the nitride film, which have appeared to have degraded passivation of Si-SiO₂ interface.

Charge density on PECVD and LPCVD nitride (50 nm) samples were measured by preparing saw damage etching n-type 1-2 $\Omega\text{-cm}$ $\langle 100 \rangle$ 250 μm thick single-sided polished

wafers, followed by RCA clean and HF dip prior to PECVD and LPCVD nitride deposition on the polished side of corresponding samples. Following the deposition of nitride films, metal-insulator-semiconductor structures were formed by depositing aluminium dots ($\sim 700 \mu\text{m}$ diameter). Gallium indium paste was then applied on the bare silicon bulk to make electrical contacts, followed by the measurement of Quasistatic (QS) and high-frequency (HF) C-V measurements. Figure 4 shows measured charge densities of PECVD and LPCVD nitride. As in figure 4, charge density in LPCVD nitride are at least 3 times higher than that in PECVD nitride.

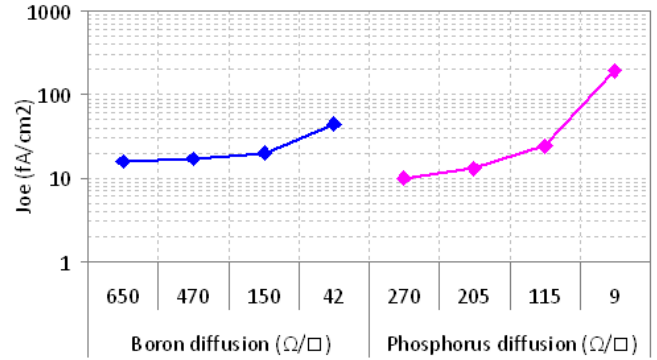


Figure 3. J_{oe} of oxide passivated boron and phosphorus diffused samples. J_{oe} represents single-sided value. Phosphorus diffusion R_{sh} is decreased from 42 to 9 Ω/\square following boron diffusion as more phosphorus ions are activated.

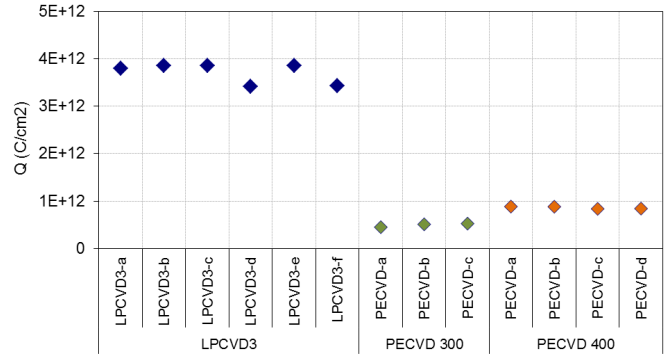


Figure 4. Positive charges measured on PECVD and LPCVD nitride films by capacitance voltage (CV) measurement. Data in x-coordinate represent amount of charges measured at individual samples.

Whether high positive charges in nitride films are the cause of surface recombination increase is further confirmed by the application of negative corona charges on boron samples with oxide and PECVD nitride layers. Following the corona charge, J_{oe} of these samples have reduced by two orders of magnitude compared to that after PECVD nitride deposition (Figure 5). These results confirm that good passivation of Si-SiO₂ interface can be maintained by depositing nitride layers with reduced positive charge [11]. Alternatively, PECVD SiO_x can

be used as a capping layer in replace of nitride. Additionally, passivation on etch-back diffusions can be improved further with an appropriately charged dielectric layer.

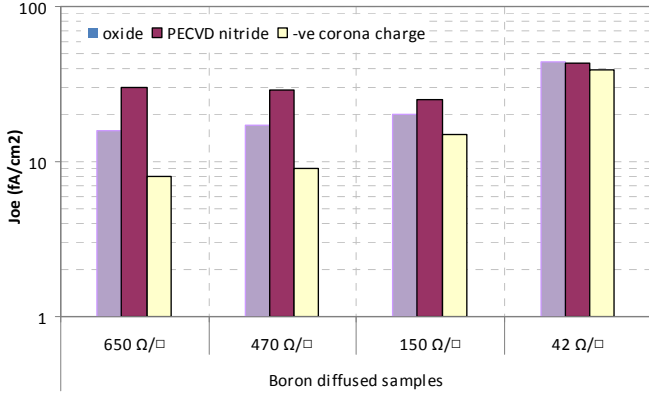


Figure 5. J_{oe} of boron-diffused samples following oxide, PECVD nitride and corona charge. J_{oe} of those samples are measured at a carrier injection of $5 \times 10^{15} \text{ cm}^{-3}$.

III. CELL STRUCTURE

Etch-back assisted IBC Si solar cell has a substrate thickness of $200 \mu\text{m}$. The front of the cell features textured surface with a passivation dielectric (PECVD SiN_x), while the rear has interdigitated light phosphorus (n) and boron (p) sheet diffusions with localized heavy p^+ and n^+ contact dots in corresponding sheet diffusions. Metals are contacted to the localized dot diffusions through the dielectric stack (thermal oxide and PECVD SiO_x) in interdigitated patterns.

IV. CELL PROCESS

Fabrication begins with saw-damage etching the $1 \Omega\cdot\text{cm}$ $300 \mu\text{m}$ thick n-type FZ wafers. Wafers are then subjected to a phosphorus tube diffusion ($\sim 40 \Omega/\square$) with in-situ oxide growth on both front and rear surfaces. Next LPCVD nitride ($\sim 50 \text{ nm}$) is deposited on the entire wafer. A pattern of boron diffusion regions are lithographically defined, followed by subjecting the patterned regions to etching in tetramethylammonium hydroxide (TMAH), which removes about $2\text{-}3 \mu\text{m}$ depth of silicon. Boron diffusion with insitu oxide ($\sim 45 \Omega/\square$) is then

formed in tube furnace to create junctions. Patterns featuring thousands of $25 \mu\text{m}$ diameter dots with a pitch of $70 \mu\text{m}$ are lithographically transferred into interdigitated boron and phosphorus diffusions, subsequently etching exposed oxide and nitride by Reactive Ion Etch (RIE). Then exposed diffusions are etched in TMAH at a temperature of 50°C for 15 minutes. This etch-back creates p, p^+ , n, n^+ diffusion simultaneously, as shown in figure 6. Next a thin oxide is grown in hot nitric acid (100°C for 30 min, followed the growth of LPCVD nitride ($\sim 15 \text{ nm}$). A stack of oxide and LPCVD nitride at the front is then etched off by hydrofluoric (HF) acid fuming, followed by random pyramidal texturing. Then all masking dielectric are stripped off, and thermal oxide ($\sim 20 \text{ nm}$) is grown on the samples, and PECVD SiO_2 ($\sim 200 \text{ nm}$) is deposited subsequently at the rear. Oxide at the front surface is removed by HF fuming and PECVD SiN_x ($\sim 80 \text{ nm}$) [12] is then passivated. Metal contacting regions are created on $\sim 200 \text{ nm}$ PECVD SiO_x by lithographic mean featuring thousands of $5 \mu\text{m}$ diameter dots with a pitch of $70 \mu\text{m}$. Aluminium ($\sim 3 \mu\text{m}$) is then deposited to blanket the rear of the cell. Interdigitated metal fingers are then formed by etching the aluminium off, following the final metal lithography patterning.

V. RECOMBINATION PARAMETERS

TABLE I. RECOMBINATION PARAMETERS OF TEST STRUCTURES MADE BY A SIMPLIFIED ETCH-BACK TECHNIQUE FOR IBC CELL.

Recombination parameters (J_{oe}) extracted out of IBC solar cell					
Diffusion	Area	ρ_{sq} (Ω/sq)	J_{0E} (fA/cm^2)	J_{0I} (fA/cm^2)	Fraction
No diff Front (100%)	100%	-	5	5	19%
N diff - Rear	32%	270	10	3	12%
N+ diff - no contact	2.20%	19	175	4	15%
N+ diff - contact	0.20%	19	280	1	2%
P+ diff - no contact	5.00%	42	45	2	9%
P+ diff - contact	0.40%	42	380	2	6%
P diff - Rear	61%	650	16	10	37%
TOTAL				26	

Recombination parameter, J_{oe} of individual diffused and undiffused regions are extracted from diffusion dummies included in the cell process. Area-weighted recombination current, J_{0I} are then deduced from the device structure and J_{oe}

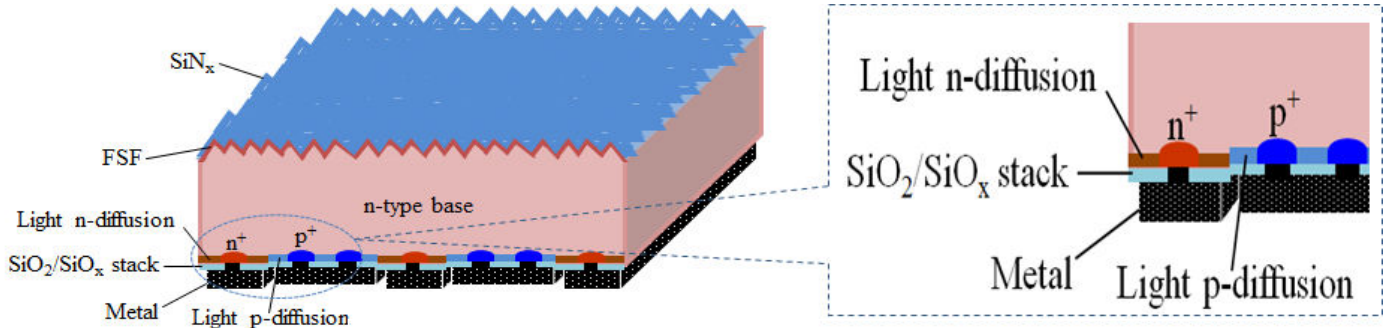


Figure 6. The structure of IBC solar cell made by simplified etch-back technique.

parameter extracted. Table 1 illustrates the J_{oe} and area-weighted J_{01} parameters of the IBC cell that can be achieved, using the technique of simplified etch-back.

VI. SIMULATION

Quokka [13] (a free and fast computer simulation program for modeling solar cells in 1D, 2D or 3D) was used to identify diffusion lateral resistance losses, as diffusion (especially boron) used for EB-IBC cells are significantly light. The reduction in fill factor (FF) is found to be in the range between 0.004 and 0.0045 when compared between 150 and 650 Ω/\square of boron diffusion. However, EB-IBC will benefit the performance gain, as open-circuit voltage increase ($\geq 10\text{mV}$), as compared to that of the IBC cell that ANU developed to date due to reduced surface recombination outweighs the reduction in FF, even with the simplification.

VII. CONCLUSION

The novel simplified technique of simultaneous etch-back to create light (n and p) and localised heavy (n^+ and p^+) diffusions is presented. The simplified technique leading to a new process offers key benefits of notable reduction in process step, compared to the process of the same device [1]; low thermal budget process, leading to possible increased in

substrate bulk lifetime and reduced contamination; and potential for higher conversion efficiency due to reduction in surface recombination. Recombination parameters from test structures and 3-dimensional simulation indicate that cells made from EB-IBC could potentially increase the performance, despite the simplified process. Next step is to finalize making cells out of this technique. Besides, outstanding surface recombination performances have been achieved with the incorporation of aluminum oxide (Al_2O_3) passivation layer on the rear (boron and phosphorus diffusions) of the cell, the results of which will be presented in other publications.

ACKNOWLEDGEMENTS

The funding of this research is supported by the Australian Solar Institute (now known as Australian Government through the Australian Renewable Energy Agency, ARENA). Responsibility for the views, information or advice expressed herein is not accepted by the Australian Government. The inductive-coupled reactive ion etching (ICP-RIE) tool used in this work is supported by the Australian National Fabrication Facility (ANFF) ACT node.

REFERENCES

- [1] A. Blakers, K. C. Fong, E. Franklin, T. C. Kho, K. McIntosh, Y. Wan, *et al.*, "24.6% efficient back contact cell with oxide - nitride passivation," in *23rd International Photovoltaic Science and Engineering Conference*, Taipei, 2013, pp. 2-5.
- [2] M. Aleman, J. Das, T. Janssens, B. Pawlak, N. Posthuma, J. Robbelein, *et al.*, "Development and Integration of a High Efficiency Baseline Leading to 23% IBC Cells," *Energy Procedia*, vol. 27, pp. 638-645, // 2012.
- [3] C. Reichel, F. Granek, M. Hermle, and S. W. Glunz, "Back-contacted back-junction n-type silicon solar cells featuring an insulating thin film for decoupling charge carrier collection and metallization geometry," *Progress in Photovoltaics: Research and Applications*, vol. 21, pp. 1063-1076, 2013.
- [4] R. Peibst, N.-P. Harder, A. Merkle, T. Neubert, S. Kirstein, J. Schmidt, *et al.*, "High-Efficiency RISE-IBC Solar Cells: Influence of Rear Side-Passivation on PN Junction Meander Recombination," in *28th European PV Solar Energy Conference and Exhibition*, Paris, 2013.
- [5] P. J. Cousins, D. D. Smith, L. Hsin-Chiao, J. Manning, T. D. Dennis, A. Waldhauer, *et al.*, "Generation 3: Improved performance at lower cost," in *Photovoltaic Specialists Conference (PVSC), 2010 35th IEEE*, 2010, pp. 000275-000278.
- [6] D. D. Smith, P. J. Cousins, A. Masad, A. Waldhauer, S. Westerberg, M. Johnson, *et al.*, "Generation III high efficiency lower cost technology: Transition to full scale manufacturing," in *Photovoltaic Specialists Conference (PVSC), 2012 38th IEEE*, 2012, pp. 001594-001597.
- [7] K. C. Fong, K. Teng, K. R. McIntosh, A. W. Blakers, E. Franklin, N. Zin, *et al.*, "Optimisation of Diffusion and Contact for IBC Solar Cells," in *28th European PV Solar Energy Conference and Exhibition*, Paris, France, 2013.
- [8] J. Nakamura, K. Kimoto, N. Asano, T. Hieda, N. Koide, H. Katayama, *et al.*, "Development of Hetero-Junction Back Contact Si Solar Cells toward the conversion efficiency of 25%," in *23rd International Photovoltaic Science and Engineering Conference*, Taipei, 2013.
- [9] Available: <http://panasonic.co.jp/corp/news/official.data/data.dir/2014/04/en140410-4/en140410-4.html>
- [10] N. S. Zin, A. Blakers, and K. Weber, "RIE-induced carrier lifetime degradation," *Progress in Photovoltaics: Research and Applications*, vol. 18, pp. 214-220, 2010.
- [11] N. M. Nursam, Y. Ren, and K. J. Weber, "PECVD Silicon Nitride Passivation on Boron Emitter: The Analysis of Electrostatic Charge on the Interface Properties," *Advances in Optoelectronics*, 2010.
- [12] W. Yimao, K. R. McIntosh, A. F. Thomson, and A. Cuevas, "Low Surface Recombination Velocity by Low-

Absorption Silicon Nitride on c-Si," *Photovoltaics, IEEE Journal of*, vol. 3, pp. 554-559, 2013.

[13]A. Fell, "A free and fast 3D/2D solar cell simulator featuring conductive boundary and quasi-neutrality

approximations," *IEEE Transactions on Electron Devices*, vol. 60, pp. 733-738, 2012.